Available online at www.sciencedirect.com
SCIENCE DIRECT®
Journal of Power Sources 123 (2003) 222–229
JOURNAL OF POWER SOURCES
www.elsevier.com/locate/jpowsour

Complexation of poly(vinylidene fluoride):$LiPF_6$ solid polymer electrolyte with enhanced ion conduction in 'wet' form

Chin-Yeh Chiang, Y.J. Shen, M. Jaipal Reddy, Peter P. Chu*

Department of Chemistry, National Central University, Chung-Li 32054, Taiwan

Received 7 March 2003; accepted 26 March 2003

Abstract

Poly(vinylidene fluoride) (PVDF):$LiPF_6$ complex membranes as 'solid' and 'wet' polymer electrolytes are evaluated. X-ray diffraction (XRD) and differential scanning calorimetric (DSC) studies show a decrease in crystalline size and crystallinity of the polymer PVDF with increasing $LiPF_6$ concentration. Although PVDF is not an ionomer, acid–base complexation between the PVDF polymer at fluorine sites and the Li ions of the $LiPF_6$ salt is evident from X-ray photoelectron spectroscopy (XPS) spectra. Such interaction is responsible for the reduction in both PVDF crystallinity and sol particle size during solid film formation. As evident from scanning electron micrographs, smaller spherical domains in the dry film are found with increasing lithium salt. Impedance (ac) measurements suggested the ionic conductivity of PVDF:$LiPH_6$ film increases with increasing lithium salt. By comparison, PVDF:$LiPH_6$ solid polymer electrolyte (SPE) wetted with Ethylene carbonate/propylene carbonate (EC/PC) shows less dependence of conductivity on salt concentration with a shallow maximum at about 15 wt.% salt. The average value is comparable with that of the solvent-free film at 20 wt.% $LiPF_6$. This result suggests the existence of dual conduction mechanisms in 'wet' SPE via the amorphous PVDF matrix and the EC/PC solution trapped in the swollen region of the PVDF porous network.

Keywords: Poly(vinylidene fluoride); Complex membranes; Polymer electrolyte; Lithium battery; Ionic conductivity

1. Introduction

Solid electrolyte materials have attracted growing interest in recent years because of their potential application at ambient temperature in ionic devices such as secondary batteries and fuel cells [1–4]. Ion conduction is an important characteristic in developing these materials. The particular advantages of polymer electrolytes over other solid electrolytes are unique mechanical and electrical properties, ease of fabrication into films of desirable sizes, and interactions to strengthen the electrode–electrolyte contact. Extensive work has been carried out on solid polymer electrolytes based on poly(ethyl oxide) (PEO) that includes its modification by plasticization and by adding inorganic oxides etc. as fillers [5–15]. Polymers such as poly(acrylonitrile) (PAN), poly(methyl methacrylate) (PMMA) and poly(vinylidene fluoride) (PVDF) have been examined as gel-type polymer electrolytes in energy-storage devices [16–21]. At present, the majority of lithium batteries uses some form of gelated PVDF electrolyte. Modifications of PVDF-based polymer electrolytes have been explored by blending with PMMA, and poly(vinyl alcohol-co-vinyl acetate) (PVAAc) [22–25]. The physical properties of polymer electrolytes are largely affected by the molecular arrangement and chemical dynamics of polymer chains. An understanding of the interplay between molecular structure and the ion transport mechanism is critical to the development of new polymer electrolyte materials.

In spite of the industrial importance and wide application of gelated PVDF, the ion conduction mechanism remains unresolved. PVDF, which has a strong electron withdrawing function and an unique arrangement, delivers a high dielectric constant ($\varepsilon = 8.4$). This is effective in dissociating lithium salt to generate a large quantity of charge carriers for conduction. It is highly possible that apart from the diffusion established by a plasticizer such as ethylene carbonate (EC), propylene carbonate (PC) or dimethyl carbonate (DMC), conduction through the swollen PVDF matrix is also highly plausible. The objective of this research is to study the morphology, structure and ion conductivity of a PVDF electrolyte membrane with lithium salt incorporated during film formation. The results are compared

* Corresponding author. Tel.: +886-3-425-8631; fax: +886-3-422-7664.
E-mail address: pjchu@cc.ncu.edu.tw (P.P. Chu).

0378-7753/$ – see front matter © 2003 Elsevier Science B.V. All rights reserved.
doi:10.1016/S0378-7753(03)00514-7

with those for a "wetted" PVDF film in order to assess possible structural factors that contribute to ion conduction. The uniqueness of this wet polymer electrolyte compared with gel-type electrolyte is that lithium ions are already planted the amorphous region of the polymer; in a gel-type electrolyte, lithium ions are introduced by the organic solvent.

2. Experimental

Solid polymer electrolyte films were synthesized by using poly (vinylidene fluoride) (PVDF) (Ploy Science, MW = 6×10^4) and $LiPF_6$ (Across). Initially, polymer PVDF was dissolved in *N*-methyl-2 pyrrolidon (NMP) followed by the addition of various amounts of $LiPF_6$ salt and stirring for 24 h at 60 °C. The homogeneous mixtures were poured on Teflon dishes and evaporated slowly at 50 °C, then dried in vacuum. Further drying was achieved in a dry box under a nitrogen atmosphere to remove traces of NMP solvent. All measurements were carried out in a nitrogen environment to avoid attack by moisture. The wetted polymer electrolyte was prepared by impregnating PVDF:$LiPF_6$ complexed film with organic EC/PC solution of 1:1 mole ratio for 10 min.

X-ray diffraction (XRD) patterns were recorded on a Shimadzu X-ray diffractometer (XRD 6000) in the range 5–60° with a scanning rate of 2°/min. Differential scanning calorimetry (DSC) studies were performed by means of a Perkin-Elmer (DSC 7 series) system at a heating and cooling rate of 10 °C/min. The weights of these samples were maintained in the range of 6–9 mg and all experiments were carried under a flow of nitrogen. Perkin-Elemer TGA-7 series equipment was used to conduct thermogravimetric analysis (TGA) in the range of 30–900 °C.

The surface morphology of such electrolytes were studied by the scanning electron microscopy (SEM) using a Hitachi (model 3500N) instrument with gold-sputtered coated films. X-ray photoelectron spectroscopy (XPS) experiments were performed in an ultra-high vacuum using a VG-Scientifica (ESCA) X-ray photoelectron spectrophotometer and an Al Kα as X-ray beam source.

Impedance spectroscopy was used to determine the ionic conductivity of the polymer electrolyte films. Measurements were carried out over the frequency range 1 MHz to 10 Hz, with the help of a frequency response analyzer, i.e. an AUTOLAB/PGSTAT 30 (potential/galvanostat) electrochemical instrument. These measurements were made over the temperature range 298–373 K, and the system was allowed to reach thermal equilibrium at each selected temperature for 30 min. The frequency response analyzer (FRA software) was used to determine the bulk resistance (R_b) within an error of below 1%. The conductivity values (σ) were calculated from the equation: $\sigma = (1/R_b)(t/A)$, where t is the thickness and A the area of the sample.

3. Results and discussion

3.1. X-ray diffraction

XRD spectra recorded for the PVDF:$LiPF_6$ solid polymer complex films are shown in Fig. 1. Sharp diffraction peaks appear at $2\theta \sim 18.7$ and 20.5° and illustrate the various crystalline forms of PVDF. Few differences are observed between the pure PVDF with that of $LiPF_6$ salt PVDF blend films. The clear and sharp crystalline diffraction peaks in pure PVDF, however, become less prominent in presence of the salt. The decrease in intensity and gradual broadening of the diffraction peaks with salt concentration, suggests a decrease in both crystalline size and the degree of crystallinity of PVDF. Although PVDF is not an ionomer, the highly depolarized CF bond is capable of forming a weak acid-based complexation with lithium, and thus retards the ordering of crystalline PVDF. The absence of corresponding lithium salt diffraction peaks in complexed polymer PVDF films indicate homogeneous distribution of the stoichiometric ratio through the complexed films which are under investigation.

3.2. Differential scanning calorimetric studies

Differential scanning calorimetry also demonstrated a loss in the long-range order of PVDF in the presence of lithium salt. DSC curves of pure PVDF and PVDF:$LiPF_6$ films are depicted in Fig. 2A and B for two heating scans. Except for pure PVDF, a re-crystallized peak is apparent (the exotherm prior to the melting temperature) for all compositions of lithium salt blend PVDF films during the first scan of endothermic. This is absent in the second scan. This peak shifts towards lower temperatures with increasing salt content (see Fig. 2A). This behavior suggests that additional PVDF crystallization occurs in freshly-prepared PVDF:$LiPF_6$ complex films upon heating at elevated temperature, possibly by driving the salt out of the amorphous PVDF domain. In

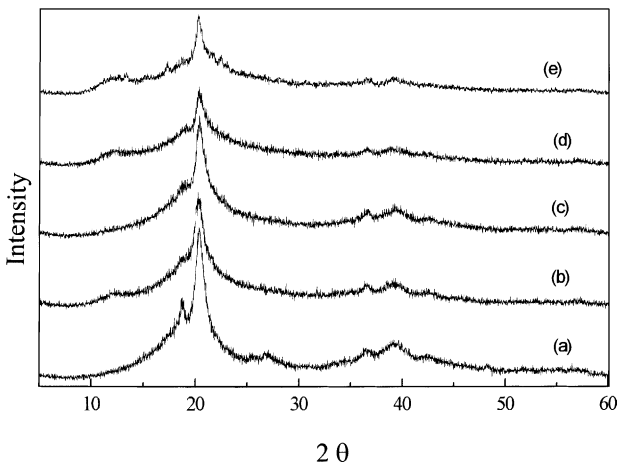

Fig. 1. X-ray diffraction spectra of (a) 0, (b) 5, (c) 10, (d) 15 and (e) 20 wt.% $LiPF_6$ salt in PVDF.

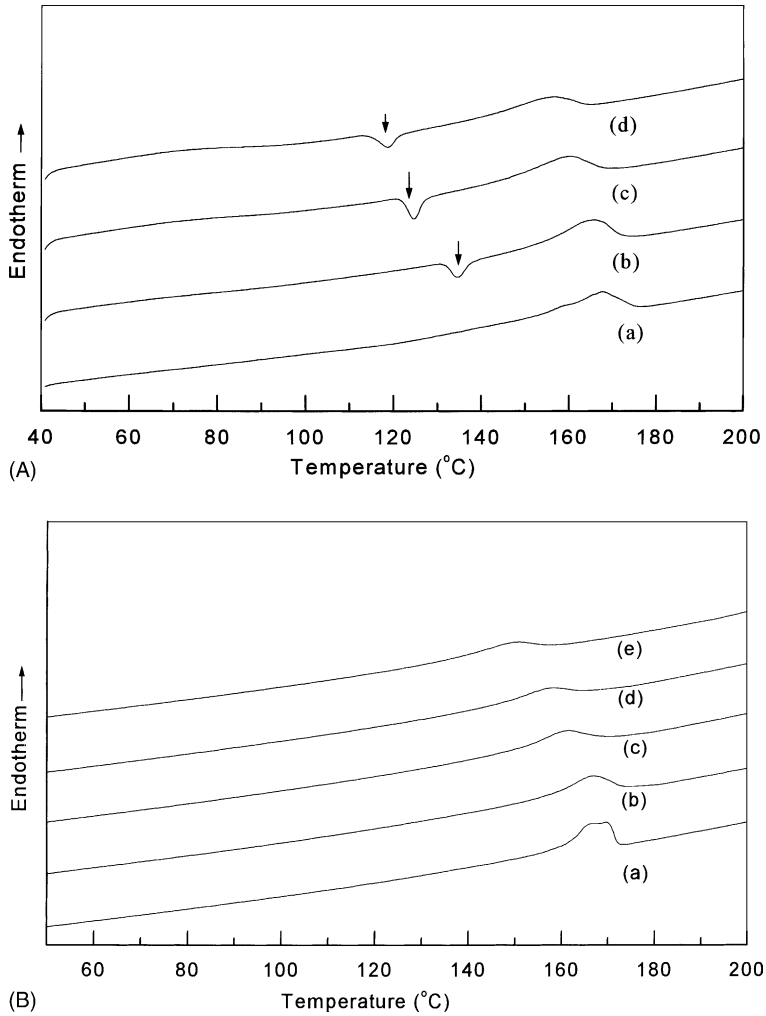

Fig. 2. (A) First scan DSC curves of (a) 0, (b) 5, (c) 10, and (d) 15 wt.% $LiPF_6$ salt in PVDF. (B) Second scan DSC curves of (a) 0, (b) 5, (c) 10, (d) 15 and (e) 20 wt.% $LiPF_6$ salt in PVDF.

both scans, the heat of fusion (ΔH_f) and the melting temperature (T_m) of polymer PVDF decreases with increasing salt content. In addition, the melting endotherms become broader. The relative crystallinity (χ) has been calculated by assuming that pure PVDF is 100% with the equation $\chi = \Delta H_f / \Delta H_f^\circ$ (where ΔH_f° is the heat of fusion of pure PVDF and ΔH_f is related to the salt in the polymer). The crystallinity (χ), melting temperature (T_m) and crystallization temperature with cooling (T_c) are tabulated in Table 1.

Table 1
Melting temperature (T_m) crystallization temperature (T_c) and crystallinity (χ, %) of PVDF:$LiPF_6$ solid polymer electrolyte on second scan

$PVDF_6$ in PVDF (wt.%)	T_m (°C)	T_c (°C)	χ (%)
0	167.39	133.71	100
5	164.36	129.08	57.9
10	159.13	122.85	46.8
15	155.63	117.98	39.8
20	147.43	111.54	39.4

It is interesting to note that χ is suppressed in the presence of lithium ionic salt. The crystallization exotherm also shifts towards lower temperatures and broadens with increasing salt content, and disappears at salt concentration of 25 wt.%. This trend agrees with the above findings from XRD curves.

3.3. Thermogravimetric analysis (TGA)

The TGA plots of the PVDF:$LiPF_6$ polymer electrolyte system are shown in Fig. 3. The thermal decomposition temperature is determined from the differential curve, and is about 500 °C for pure PVDF (see Fig. 3a). The absence of weight losses prior to polymer melting indicates no impurity such as solvent, water, etc. is present, and confirms that drying under vacuum and nitrogen gas is efficient. The degradation temperature decreases continuously with increasing addition of $LiPF_6$ to PVDF, a result directly related to an increase in the amorphous fraction of the electrolyte. The thermal stability of the polymer is reduced with the

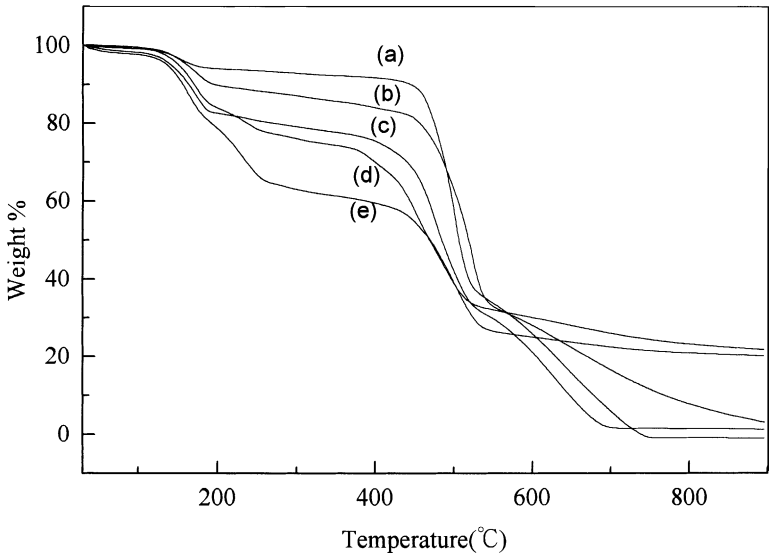

Fig. 3. TGA plots of (a) 0, (b) 5, (c) 10, (d) 15 and (e) 20 wt.% $LiPF_6$ salt in PVDF.

addition of ionic salts due to the growth of the amorphous fraction, which is a typical characteristic of polymers. A higher fraction of residue above 500 °C is found with increasing salt. The source of the incomplete decomposition at high salt content is not clear, but is believed to be associated with the PF_6 anion containing backbone.

3.4. Scanning electron micrograph

Scanning electron micrographs of PVDF:$LiPF_6$ films are displayed in Fig. 4. The surface structure of pure PVDF shows connecting spherical domains with a reversed pore shape (see Fig. 4a). As PVDF is a polymer with a high

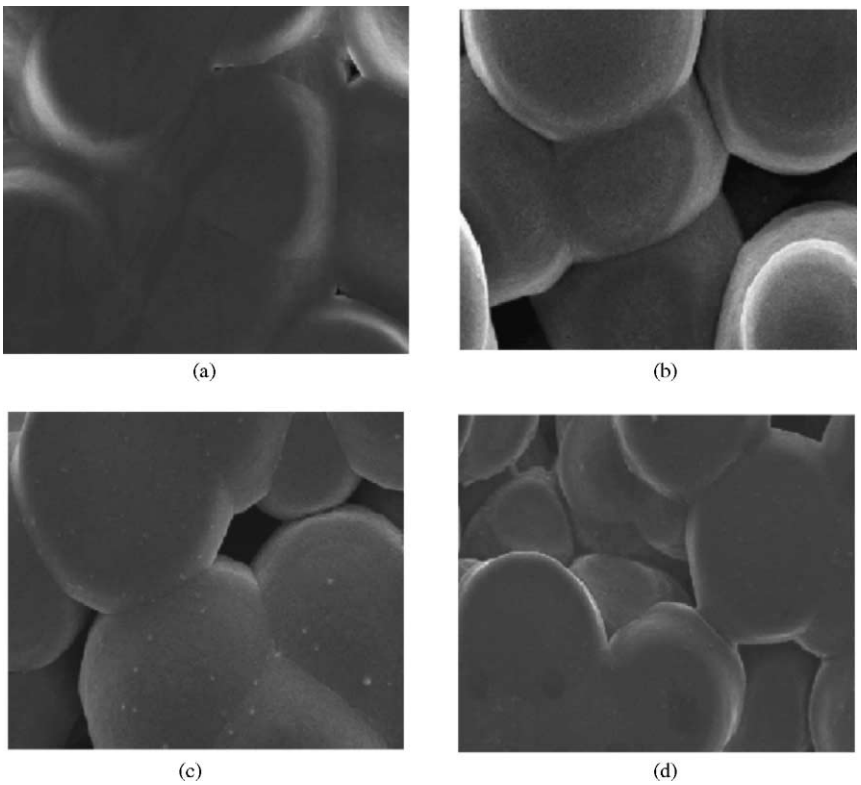

Fig. 4. Scanning electron micrograph (1000×) of (a) 0, (b) 5, (c) 10 and (d) 20 wt.% $LiPF_6$ salt in PVDF.

dielectric constant, the surface tension is also high. Sol formation is necessary in the process of drying solvent from the miscible solution or heterogeneous gel solution. The size of the spheres and the morphology in the dry PVDF film is thus highly dependent upon the preparation conditions such as the solvent and the temperature. On addition of $LiPF_6$ to PVDF, the acid–base interaction not only changes the crystallinity but also reduces the surface potential, and the equilibrium sol dimension becomes smaller. As seen from Fig. 4b–d, the spherical shape domains are smaller in size compared with pure PVDF and still have spherical shapes with improved smoothness. A plausible PVDF structure on the surface is an amorphous polymer chain which is physically cross-linked by the dissociated Li^+ and PF_6^- ions through coordination with polymer fluorine.

3.5. XPS analysis

Although DSC, XRD, SEM results demonstrate the interaction between lithium ionic salt and PVDF polymer, clear evidence of complex coordination can be obtained from the XPS technique. The XPS spectra were obtained in the range 0–800 eV. The major peaks identified in the electrolyte films are for carbon (C) 1s, fluorine (F) 1s and $2s_{1/2}$, and lithium (Li) 1s.

The C 1s spectra of pure PVDF and of PVDF complexes with $LiPF_6$ salt are presented in Fig. 5. The pure PVDF C 1s spectrum consists of two major peaks at 290.2 and 285.6 eV, which correspond to CF_2 and CH_2 groups, respectively. In presence of lithium salt, the C 1s spectrum broadens and also shifts to 290 and 285.1 eV. The shift of the C 1s spectrum in both groups and the broadening suggests that lithium ion may be interacting with fluorine in the PVDF.

The F 1s and F $2s_{1/2}$ signals of pure PVDF and the lithium salt complexed PVDF polymer are shown in Fig. 6A and B. The PVDF F 1s and F $2s_{1/2}$ spin-orbital splitting photoelectrons for pure PVDF are located at binding energies of 687.5 and 32.6 eV, respectively. In F 1s (Fig. 6A) spectra the

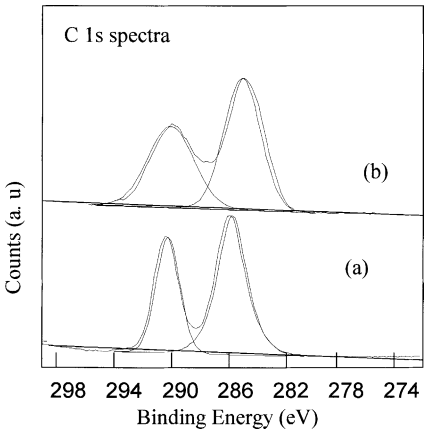

Fig. 5. XPS spectra of C 1s region: (a) pure PVDF; (b) 10 wt.% $LiPF_6$ in PVDF.

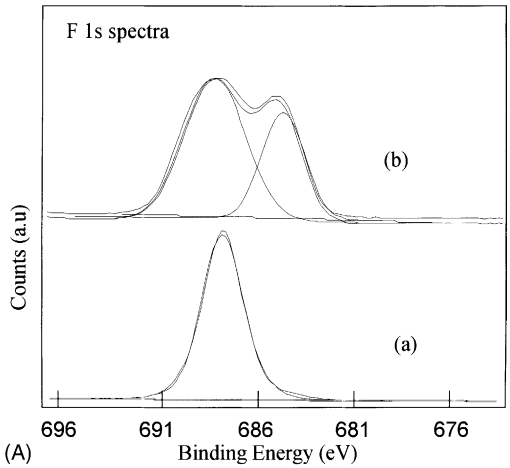

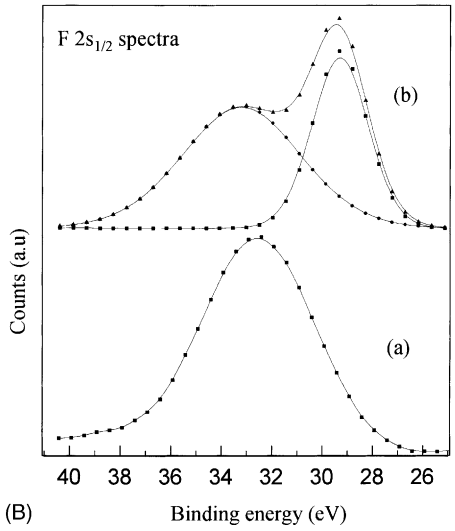

Fig. 6. (A) XPS spectra of F 1s region: (a) pure PVDF; (b) 10 wt.% $LiPF_6$ in PVDF. (B) XPS spectra of F $2s_{1/2}$ signal: (a) pure PVDF; (b) 10 wt.% $LiPF_6$ in PVDF.

CF binding energy is shifted 0.5 eV (to 688 eV) and a strong new peak appears at 684.8 eV. This gives clear indication of Li coordination with the F atom. In the F $2s_{1/2}$ spectra region (Fig. 6B) two binding peaks (33.6 and 29.4 eV) were identified as lithium salt complexed to PVDF. It is difficult to conclude whether this additional peak (29.4 eV) entirely originates from lithium coordination with the PF_6 anion or with the fluorine atom from PVDF. Nevertheless, the shift to higher binding energy and the broadening of the spectra in PVDF complexed with salt already indicates lithium interaction with fluorine sites in polymer.

The Li 1s XPS spectra in the range 51–58 eV for pure PVDF and PVDF complexed with $LiPF_6$ films are given in Fig. 7. A broad peak with highest intensity at 54.9 eV is apparent in the $LiPF_6$ added PVDF polymer film, where no such peak in pure PVDF film is found. This peak appears in all the salt-added PVDF films, and broadens further with increasing addition of lithium salt. This result also supports lithium coordination with PVDF polymer. Complexation in

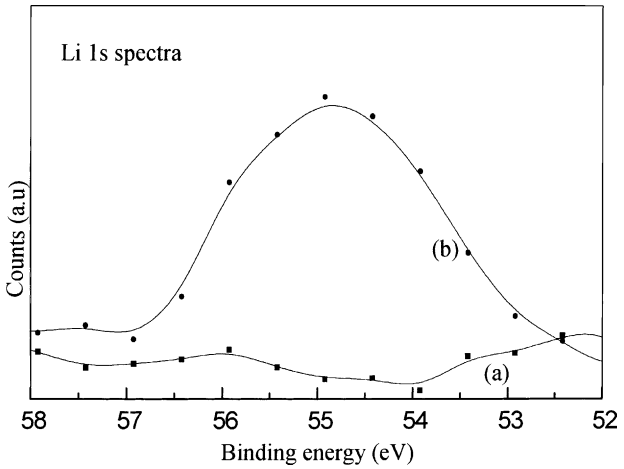

Fig. 7. XPS spectra of Li 1s signal: (a) pure PVDF; (b) 10 wt.% $LiPF_6$ in PVDF.

the PVDF:$LiPF_6$ polymer accounts for the reduced PVDF crystallinity and the changes in morphology with increasing lithium salt. A plausible complex structural model of PVDF with $LiPF_6$ is presented in Fig. 8.

3.6. Conductivity

The dependence of conductivity (σ) on temperature is depicted in Fig. 9. Conductivity data at room temperature are summarized in Table 2. Interestingly, the conductivity of the complex PVDF dry films increases continuously with $LiPF_6$ content at all temperatured measures. This behavior is different from that of PEO solid polymer electrolyte systems, where a maximum conductivity is identified at particular compositional ratio [10,26–29]. In this case, incomplete dissociation and the formation of triplets at higher salt content are responsible for the reduced conductivity. The ion-paring mechanism appears to be absent in the PVDF polymer electrolyte films studied here, due to the high dielectric constant of the medium.

The plot of $\log\sigma$ versus $1000/T$ follow an Arrhenius-type, thermally-activated process. The conductivity relationship can be expressed as $\sigma = \sigma_0 \exp(-E_a/kT)$, where σ_0 is the pre-exponential factor, E_a the activation energy and k the Boltzman constant. Activation energies of PVDF:$LiPF_6$ solid polymer electrolytes are evaluated by linear fitting, the results are listed in Table 2. It is found that the activation energy decreases with increasing salt concentration in polymer PVDF.

Druger et al. [30,31] have attributed the change in conductivity with temperature in solid polymer complexed systems to segmental (i.e. polymer chain) motion, which results in an increase in the free volume of the system. Thus, the segmental motion either permits the ions to hop from one site to another or provides a pathway for ions to move. In other words, the segmental movement of the polymer facilitates the transitional ionic motion. From this, it is clear that the ionic motion is due to ionic transitional motion/hopping facilitated by the dynamic segmental motion of the polymer. As the amorphous region increases, however, the polymer chain acquires faster internal modes in which bond rotations produce segmental motion to favor inter- and intra-chain ion hoping, and thus the degree of conductivity becomes high.

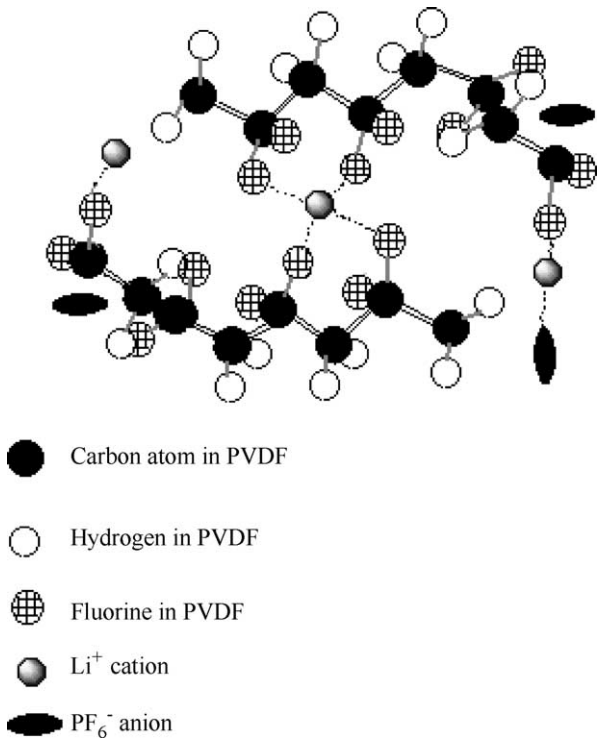

Fig. 8. Plausible structural model of PVDF:$LiPF_6$ complex electrolyte.

4. Plasticizer EC/PC effect

Plasticizer, which fills the pores and swells the polymer matrix is adopted to enhance the conductivity of PVDF:$LiPF_6$ solid polymer electrolyte. The isothermal ion conductivity of plasticized ('wet') polymer electrolyte PVDF:$LiPF_6$ along with dry ('solid') polymer electrolyte at room temperature are shown in Fig. 10. The conductivity and EC/PC uptake data are given in Table 2. The results show that the ion conductivity of the 'wet' electrolyte is less dependent on the salt concentration. The conductivity is three orders higher in 'wet' electrolyte at low $LiPF_6$, compositions, but becomes comparable with that of the dry film when the salt content reaches 20 wt.%. Note that, present wet membranes are achieved by slight immersion in EC/PC solution. This is a different process from that for gel-type electrolytes in which the pure polymer film is gelated in the electrolyte solution. The advantage of the present preparation is that lithium ions are already planted in the solid network polymer matrix and are not supplied by

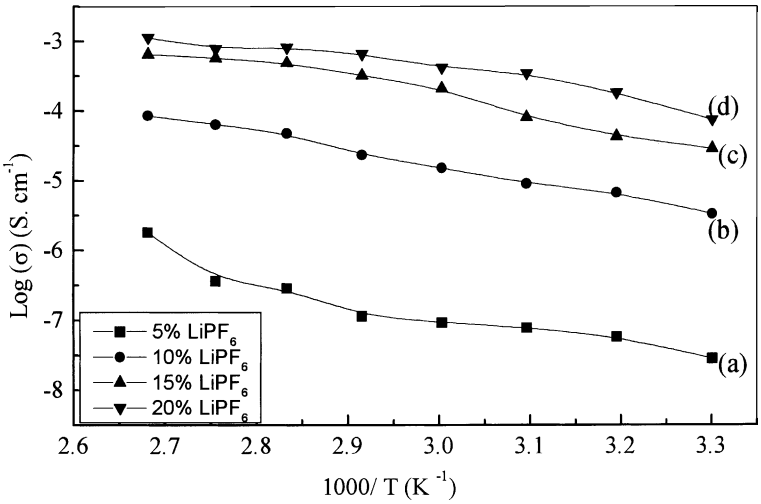

Fig. 9. Conductivity vs. temperature plots of (a) 5, (b) 10, (c) 15 and (d) 20 wt.% $LiPF_6$ salt complex in PVDF solid polymer electrolyte system.

Table 2
Room-temperature conductivity ('solid' and 'wet' forms), activation energies, and EC/PC uptake of PVDF:$LiPF_6$ electrolyte

$LiPF_6$ in PVDF (wt.%)	Conductivity in solid form (S cm^{-1})	Activation energy in solid form (E_a, eV)	Conductivity in wet form with EC/PC (S cm^{-1})	EC/PC uptake by film (wt.%)
5	8.46×10^{-8}	0.21	1.46×10^{-4}	25
10	2.34×10^{-6}	0.20	5.0×10^{-4}	27
15	2.10×10^{-5}	0.20	5.6×10^{-4}	25
20	2.70×10^{-4}	0.15	1.9×10^{-4}	24

the gel electrolyte solution. The EC/PC solution penetrates the pores of the solid polymer electrolyte network, which occupies the pore space within the swollen polymer chain.

The results suggest that charge migration in wet polymer electrolyte originates from multiple (possibly coupled) mechanisms; i.e. ion transport through the swollen polymer via diffusion of small EC/PC molecules, and via the solid polymer network region.

In the present wet electrolyte membranes, lithium ions influence the polymer because the species are within the vicinity of the polymer chains and can be affected by the swollen polymer network. This differs from the situation in gel-type polymer electrolytes, which undergo little interaction with the polymer due to their remote location from the polymer chains [20]. The dissociation condition of the salt and the carrier mobility are dominated by the property of the polymer and solution. The overall ion conductivity is determined by the dissociation of salt, and ion mobility is governed by the polymer, the plasticizer dielectric constant, and the viscosity. Further investigation is in progress to identify the causes of the enhancement of the conduction mechanism in the 'wet' form of the solid polymer electrolyte.

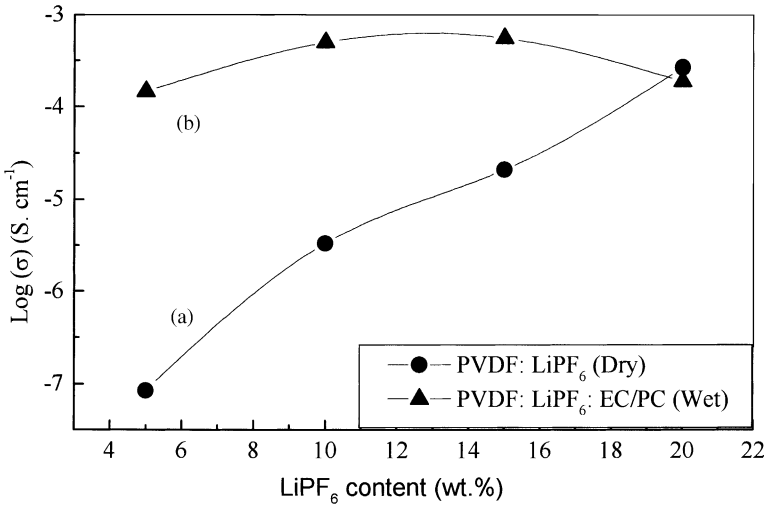

Fig. 10. $LiPF_6$ concentration dependence conductivity of (a) 'solid' and (b) 'wet' form of PVDF:$LiPF_6$ complex electrolyte.

5. Conclusions

The interaction between Li^+ ions and fluorine in the polymer effectively disrupts the crystallinity of PVDF. Of significance is the continuous in ion conductivity with increasing salt concentration. The conductivity is enhanced to three orders by plasticization with the EC/PC solution, when compared with dry SPE at 5 wt.% $LiPF_6$ composition. The conduction mechanism in wet SPE is associated with swollen polymer network chains via EC/PC molecules and also form a solid amorphous polymer region. The marked distinction of the wet polymer electrolyte from gel-type electrolytes is that lithium ions are already within the solid region of the polymer.

Acknowledgements

The authors are grateful to the National Science Council, Taiwan, for financial support under research project contract no. NSC 91-2811-M-008-010.

References

[1] P. Vashishta, J.N. Mundy, J.K. Shenoy (Eds.), Fast Ion Transport in Solids, North-Holland, Amsterdam, 1979.
[2] J.R. Mac Callum, C.A. Vincent (Eds.), Polymer Electrolyte Reviews, Elsevier, Amsterdam, 1987.
[3] B. Scrosati (Ed.), Application of Electroactive Polymers, Chapman & Hall, London, 1993.
[4] M.A. Ratner, D.F. Shriver, Chem. Rev. 88 (1988) 109.
[5] E.A. Reitman, M.L. Kaplan, R.J. Kava, Solid State Ionics 17 (1985) 67.
[6] D.P. Tunstall, A.S. Tomlin, J.R. Mac Callum, C.A. Vincent, J. Phys. C: Solid State Phys. 21 (1988) 1039.
[7] A. Patrik, M. Glasse, R. Latham, R. Linford, Solid State Ionics 18–19 (1986) 1063.
[8] J.M. Philas, B. Marsan, Electrochim. Acta 44 (1999) 2351.
[9] M.J. Reddy, P.P. Chu, Electrochim. Acta 47 (2002) 1189.
[10] P.P. Chu, H.P. Jen, F.R. Lo, C.L. Lang, Macromolecules 32 (2000) 4738.
[11] E. Morales, J.L. Acosta, Solid State Ionics 96 (1997) 99.
[12] F. Croce, G.B. Appetechi, L. Persi, B. Scrosati, Nature 373 (1995) 557.
[13] B. Kumar, L.G. Scanlon, J. Electroceram. 5 (2) (2000) 127.
[14] C.J. Leo, G.V. Subba Rao, B.V.R. Chowdari, Solid State Ionics 148 (2002) 159.
[15] P.P. Chu, M.J. Reddy, H.M. Kao, Solid State Ionics 156 (2003) 141.
[16] D. Peramunage, D.M. Pasquariello, K.M. Abraham, J. Electrochem. Soc. 42 (1995) 1789.
[17] H. Hong, C. Liquan, H. Xujie, X. Rongjan, Electrochim. Acta 37 (1992) 1671.
[18] O. Bohke, C. Frand, M. Razrazi, C. Rousselt, C. Truche, Solid State Ionics 66 (1993) 97.
[19] F. Boudin, X. Andrieu, C. Jehoulet, I.I. Olsen, J. Power Sources 81–82 (1999) 804.
[20] Y. Saito, H. Kataoka, E. Quartarone, P. Mustarelli, J. Phys. Chem. B 106 (2002) 7200.
[21] Y. Saito, H. Kataoka, A.M. Stephan, Macromolecules 34 (2001) 6995.
[22] N. Moussaif, R. Jerome, Polymer 40 (1999) 3919.
[23] Z. Jin, K.P. Pramoda, S.H. Goh, G. Xu, Mater. Res. Bull. 37 (2002) 271.
[24] G. Bauduin, B. Boutevin, P. Gramain, A. Malinova, Eur. Polym. J. 35 (1999) 285.
[25] S. Rajendran, O. Mahendran, R. Kannan, Fuel 81 (2002) 1077.
[26] S.M. Zahurak, M.L. Kaplan, E.A. Rietman, D.W. Murphy, R.J. Cava, Macromolecules 21 (1988) 654.
[27] M.A. Ratner, A. Nitzman, Faraday Discuss. Chem. Soc. 88 (1989) 19.
[28] R. Dupon, B.L. Papke, M.A. Ratner, D.H. Whitmore, D.F. Shriver, J. Am. Chem. Soc. 104 (1982) 6247.
[29] M.J. Reddy, P.P. Chu, J. Power Sources 109 (2002) 340.
[30] S.D. Druger, A. Nitzam, M.A. Ratner, J. Chem. Phys. 79 (1983) 3133.
[31] S.D. Druger, A. Nitzam, M.A. Ratner, Phy. Rev. B 31 (1985) 3939.